

## INFLUENCE OF THE ELECTRODES' DISTANCE UPON THE ELECTRICAL, OPTICAL AND STRUCTURAL PROPERTIES OF PECV-DEPOSITED HYDROGENATED AMORPHOUS SILICON FILMS FOR HETEROJUNCTION SOLAR CELL APPLICATION

Angelika Gorgulla, Nils Brinkmann, Anja Bauer, Giso Hahn, Barbara Terheiden

University of Konstanz, Department of Physics, 78457 Konstanz, Germany

Phone: +49 7531 88 2080, Fax: +49 7531 88 3895, Email: angelika.gorgulla@uni-konstanz.de

**ABSTRACT:** In order to fabricate highly efficient heterojunction solar cells a very thin ( $d < 6$  nm), but well passivating intrinsic a-Si:H film is needed as buffer layer between the crystalline silicon (c-Si) base and the doped a-Si:H emitter layer. In this work amorphous silicon films deposited by plasma enhanced chemical vapor deposition at low temperatures ( $T_{\text{dep}} < 225^\circ\text{C}$ ) are investigated in terms of their electrical, optical and structural properties in dependence of the inter-electrodes' distance by using Fourier-transform infra-red (FTIR) spectroscopy, photoconductance decay (PCD) and spectral ellipsometry (SE) measurements. Electrodes' distance is varied from 20 mm to 120 mm. Regarding the passivation quality of the a-Si:H film an optimum electrodes' distance of 60 mm correlated with a high Si-H bonding density is found. Moreover, the electrodes' distance is observed to have a large influence on the initial growth rate of (i)a-Si:H films. With increasing electrodes' distance the thickness of the fast grown layer, which forms directly after plasma ignition, decreases and therewith the overall thickness of thin intrinsic a-Si:H films. **Keywords:** a-Si:H, passivation, heterojunction solar cells, PECVD

### 1 INTRODUCTION

The heterojunction solar cell concept, which utilizes stacked films composed of an intrinsic amorphous silicon (a-Si:H) passivation and a doped a-Si:H emitter layer on top of a crystalline silicon base, has become one promising option in photovoltaics industry [1]. Its key advantages are a high conversion efficiency potential (24.7%) [2] and the possibility to fabricate the solar cell at economical and energy efficient temperatures below  $200^\circ\text{C}$  [3]. The insertion of a well passivating film of intrinsic a-Si:H between the c-Si base and doped a-Si:H emitter allows to obtain very high open-circuit voltages ( $V_{\text{oc}} > 720$  mV). As a consequence of parasitic absorption within the a-Si:H layers causing losses in the short circuit current and large serial resistance of a-Si:H leading to a reduction of the fill factor, this buffer layer is required to be very thin ( $d < 6$  nm) in order to not reduce the efficiency of the solar cell [4].

Numerous studies upon the properties of intrinsic a-Si:H films, in particular regarding passivation quality, have already been performed [5-7]. However, only little work is done with respect to the influence of electrodes' distance in a commonly used plasma-enhanced chemical vapor deposition (PECVD) setup operating in parallel-plate mode [8]-[12]. While most publications focus on growth rate, hydrogen content and nano-crystallinity of the intrinsic a-Si:H films, none of them addresses the influence of electrodes' distance on the passivation quality or on the accelerated initial growth rate during deposition of (i)a-Si:H films. Furthermore, only small electrodes' distances ranging from 4 to 50 mm have been investigated in these previous studies.

Therefore this study focuses on the influence of electrodes' distance ranging from 20 to 120 mm upon the electrical, optical and structural properties of PECV-deposited thin intrinsic amorphous silicon films with the overall goal to make these layers applicable to silicon heterojunction solar cells. The influence of electrodes' distances upon the properties of doped a-Si:H films is discussed elsewhere [13].

### 2 EXPERIMENTAL

The a-Si:H layers are manufactured using a commercial PECVD tool (PlasmaLab 100 from Oxford Instruments) in a direct plasma system operating at a radio frequency (RF) of 13.56 MHz. The a-Si:H films are grown by decomposition of silane ( $\text{SiH}_4$ ). In some cases the precursor gas is diluted with hydrogen ( $\text{H}_2$ ) with a ratio of  $[\text{H}_2]/([\text{H}_2]+[\text{SiH}_4])=2$ . Substrate temperature ( $225^\circ\text{C}$ ),  $\text{SiH}_4$  flow and gas pressure are kept constant for all depositions. Electrodes' distance is varied over a wide range from 20 up to 120 mm. All c-Si FZ wafers passivated by a-Si:H films ( $d_{\text{film}} \sim 20$  nm) are annealed on a hot plate in ambient air ( $300^\circ\text{C}$ , 2 min) to exploit the full passivation potential.

The 250  $\mu\text{m}$  thick 2  $\Omega\text{cm}$  (100)-oriented boron-doped float-zone (FZ) silicon wafers with an area of  $5 \times 5$   $\text{cm}^2$ , which are used as substrates, are prepared by standard chemical polishing [14] followed by an RCA cleaning [15]. Prior to PECV-deposition, a short dip in diluted hydrofluoric acid solution (HF, 2%) is performed in order to remove the native oxide. The characterization consists essentially of three parts: an electrical, optical and a structural analysis.

The electrical characterization, i.e. the passivation quality of the a-Si:H films, is carried out in terms of effective minority carrier lifetime  $\tau_{\text{eff}}$  of surface passivated c-Si wafers ( $d_{\text{film}} \sim 20$  nm).  $\tau_{\text{eff}}$  is determined as a function of excess carrier density by means of photoconductance decay (PCD) measurement using the lifetime tester WCT 120 from Sinton Consulting Inc. [16]. The Olibet Model [17] is used in order to determine the interface defect density  $N_s$ . For lifetime measurement, a-Si:H films are deposited on both sides of the FZ Si wafer by varying the electrodes' distance (20 - 120 nm) and without addition of hydrogen to the precursor gas. Only at an electrodes' distance of 60 mm are additionally a-Si:H layers deposited with a  $\text{SiH}_4$  to  $\text{H}_2$  ratio of 1:2.

The thickness of the deposited films  $d_{\text{film}}$  and their optical properties are deduced from spectral ellipsometry measurements between wavelengths from 250 to 1000 nm. For this purpose the  $(\psi, \Delta)$  data are fitted by a

Kramers-Kronig-consistent model [18]. The optical band gap  $E_{\text{gap}}$  is calculated from the fitted data by using Tauc's formula [19].

A qualitative bonding analysis of the a-Si:H films is performed by Fourier-transform infrared spectroscopy (FTIR). The a-Si:H film in this case is deposited on only one side ( $d_{\text{film}} > 150$  nm) in contrast to the lifetime samples.

### 3 RESULTS

#### 3.1 Fast grown layer and steady-state growth rate

Directly after plasma ignition the density of unconsumed precursor gas molecules is higher than the consumed molecules' density compared to the steadily burning plasma where the number of consumed molecules equals the number of unconsumed molecules. Consequently, the initial growth rate directly after plasma ignition is higher than the constant steady-state growth rate of the steadily burning plasma. a-Si:H deposited during the period of enhanced growth is likely to have different structural properties than steady-state grown a-Si:H and is therefore referred to as fast grown layer.

In this study, the thickness of the fast grown layer is determined at each electrodes' distance by linear fitting the entire a-Si:H film thickness in dependence of deposition time ( $t_{\text{dep}} \geq 10$  s) for several samples deposited with identical deposition parameters. The asymptotic thickness of the fast grown layer corresponds to the y-axis intercept of the linear regression of the a-Si:H film's thickness dependent on deposition time, while the slope of the linear regression corresponds to the steady-state growth rate (Fig. 1). The accelerated initial growth is characterized in terms of thickness (nm) and not in terms of rate (nm/s), since the duration of plasma ignition is not easily terminable.

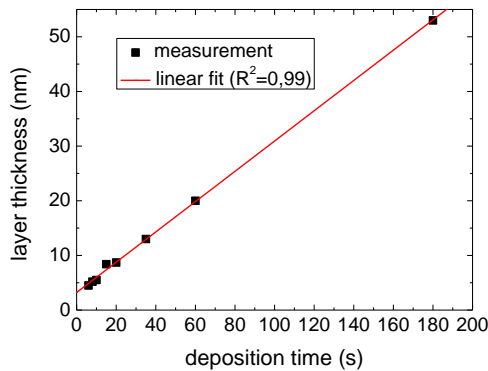


**Figure 1:** Determination of thickness of fast grown layer (y-axis intercept), which forms directly after plasma ignition, and steady-state growth rate (slope) for deposition at an electrodes' distance of 60 mm (with hydrogen added to precursor gas).

Steady-state growth rate of a-Si:H films is found to stay almost constant ( $0.3 \text{ \AA/s}$ ) for electrodes' distances larger than 40 mm and to increase for smaller electrodes' distances up to  $0.48 \text{ \AA/s}$  (Fig. 2).

The fast grown layer thickness decreases from 17.7 nm at an electrodes' distance of 20 mm to 3.5 nm at 120 mm (Fig. 2). By adding hydrogen to the precursor gas ( $[\text{H}_2]/([\text{H}_2]+[\text{SiH}_4])=2$ ), it is possible to reduce the fast

grown layer thickness at an electrodes' distance of 60 mm to 4.1 nm while maintaining a low growth rate of  $0.3 \text{ \AA/s}$  as well as a high minority carrier lifetime of the passivated FZ-Si wafer (2.9 ms, cf. Fig. 2 and 3). Hydrogen dilution is therefore advantageous for the application in heterojunction solar cells, for which the intrinsic buffer layer thickness should be less than 6 nm [4].

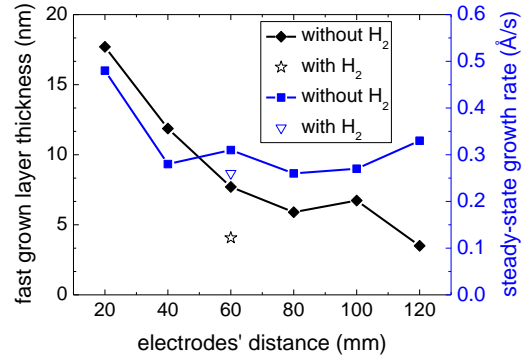


**Figure 2:** Fast grown layer thickness (black) and growth rate (blue) of deposited a-Si:H films dependent on electrodes' distance.

#### 3.2 Passivation quality

The resulting minority carrier lifetime and interface defect density dependent on the electrodes' distance are presented in Fig. 3. A maximum  $\tau_{\text{eff}}$  of 2.6 ms ( $S_{\text{eff}}=4.6 \text{ cm/s}$ ) is reached at an electrodes' distance of 60 mm. For lower and higher electrodes' distances lifetime decreases, with a sharp drop to less than 0.3 ms for an electrodes' distance of 20 mm. This drop in lifetime is accompanied by a sharp increase of  $N_s$ , which explains for all electrodes' distances the trend of minority carrier lifetime.

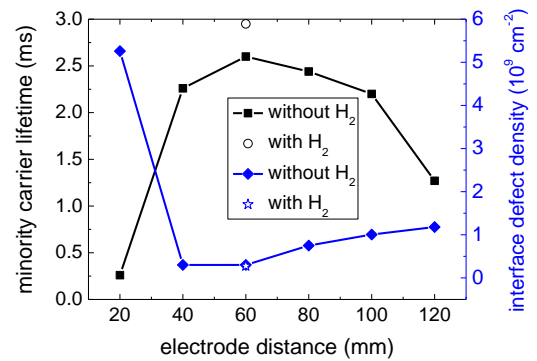


**Figure 3:** Minority carrier lifetime (black) and interface defect density  $N_s$  (blue) of deposited a-Si:H films dependent on electrodes' distance.

#### 3.3 FTIR analysis

The bonding structure of the a-S:H films is investigated using FTIR spectroscopy. Bonding densities of the Si-H bond ( $2000 \text{ cm}^{-1}$ ) and the Si-H<sub>2</sub> bond ( $2100 \text{ cm}^{-1}$ ) are determined by the FTIR measurements according to [20] and shown in Fig. 4. Whereas the Si-H<sub>2</sub> bonding density stays almost constant for an electrodes' distance above 40 mm, the Si-H bonding follows the trend of minority carrier lifetime. Therefore a correlation between the Si-H bonding density and the minority carrier lifetime can be assumed.

However, this correlation is not observed for an electrodes' distance below 40 mm, where the Si-H bonding density increases despite a sharp drop of the lifetime.

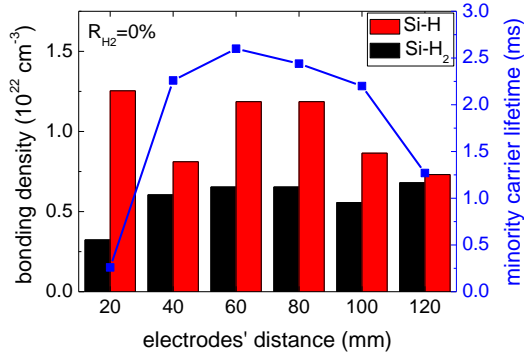


**Figure 4:** Bonding densities (Si-H, Si-H<sub>2</sub>) and effective minority carrier lifetime dependent on electrodes' distance.

### 3.4 Optical properties

Neither a correlation between refractive index  $n$  and electrodes' distance nor between energy gap  $E_{\text{gap}}$  and electrodes' distance is observed.

## 4 DISCUSSION

According to Kushner [8], the volume between electrodes in a PECVD operating in a parallel-plate configuration can be separated in two parts: the sheaths region next to the electrodes, in which power utilization occurs through higher energy processes, and the bulk plasma region, in which power utilization occurs through lower energy processes, as vibrational excitations. Sheaths regions occupy a fixed volume independent of electrodes' distance [8]. Therefore, if electrodes' distance decreases, fraction of power utilization by higher energetic processes increases. As a consequence, more SiH<sub>4</sub> is dissociated resulting in an enhanced growth rate with decreasing electrodes' distance (Fig. 2). Same argumentation applies for fast grown layer thickness. If more SiH<sub>4</sub> is dissociated at the very beginning of the deposition process, fast grown layer thickness rises.

As a result of the fixed sheaths region volume, the bombardment intensity of the c-Si wafer surface with high energetic particles rises with decreasing electrodes' distance, yielding an enhanced interface defect density and therewith a decrease in minority carrier lifetime (Fig. 3). In contrast, an increased electrodes' distance results in a larger fraction of power utilization in the plasma bulk due to lower energetic processes, which goes along with less surface bombardment with higher energetic particles.

The observed drop in minority carrier lifetime for electrodes' distances larger than 60 mm can be explained as follows: the average residence time of radicals within the plasma increases with electrodes' distance [8]. Thus, the probability of secondary chemical reactions after initial dissociation of silane increases and therewith the density of polyhydrides within the plasma. The increase of polyhydrides is reflected by an increase of the Si-H<sub>2</sub> bonding density at large electrode distance (120 mm, cf. Fig. 4). These polyhydrides are detrimental to the electronic quality of the a-Si:H film [8] and could

therefore be responsible for the decrease of minority carrier lifetime with increasing electrodes' distance.

## 5 SOLAR CELL RESULTS

Heterojunction solar cells featuring optimized intrinsic buffer layers have achieved efficiencies up to 15.8% so far ( $J_{\text{SC}} = 32.5 \text{ mA/cm}^2$ ,  $V_{\text{OC}} = 671 \text{ mV}$ ,  $\text{FF} = 72\%$ ). The manufactured heterojunction solar cells are composed of a non-textured front side, an n-type c-Si base (1  $\Omega\text{cm}$ , 500  $\mu\text{m}$ ), an n<sup>+</sup>-type a-Si:H BSF, an a-Si:H emitter stack consisting of a thin intrinsic buffer layer and a p-doped emitter layer, as well as a reactively sputtered ITO layer as transparent conductive oxide.

## 6 CONCLUSION

We have studied the influence of the electrodes' distance on the electrical, optical and structural properties of PECVD-deposited a-Si:H films.

Not only passivation quality of a-Si:H films, but also fast grown layer thickness and steady state-state growth rate depend on the electrodes' distance. Whereas thickness of fast grown layer and steady-state growth rate decrease with increasing electrodes' distance, minority carrier lifetime shows a clear maximum at an electrodes' distance of 60 mm.  $\tau_{\text{eff}}$  is directly correlated to the a-Si:H/c-Si interface defect density  $N_s$  and follows the amount of hydrogen within the films for electrodes' distances larger than 20 mm. Although a correlation of the Si-H bonding density within the films and minority carrier lifetime was found (except for the smallest electrodes' distance), no correlation has been observed between electrodes' distance and the optical properties (refractive index and bandgap) of the films. By adding hydrogen to the precursor gas it is possible to decrease the buffer layer thickness down to 4.1 nm while maintaining the high passivation quality of the films (2.9 ms).

For application in heterojunction solar cells 60 mm has been found to be the optimum electrodes' distance in terms of high minority carrier lifetime and low fast grown layer thickness. This optimum electrodes' distance can be understood as tradeoff between surface damage due to high energetic particles from the sheaths region and the amount of polyhydrides within the plasma, which are detrimental to the film quality.

Heterojunction solar cells featuring optimized intrinsic buffer layers have achieved efficiencies up to 15.8% so far.

## 6 REFERENCES

- [1] S. De Wolf, A. Descoeurdes, Z.C. Holman, C. Ballif, Green 2 (2013) 7.
- [2] Press Release: [http://www.pv-tech.org/news/recombination\\_loss\\_improvements\\_key\\_to\\_panasonic\\_hit\\_cell\\_efficiency\\_of\\_24](http://www.pv-tech.org/news/recombination_loss_improvements_key_to_panasonic_hit_cell_efficiency_of_24), date 12.02.2013.
- [3] S. Taira, Y. Yoshimine, T. Baba, M. Taguchi, H. Kanno, T. Kinoshita, H. Sakata, E. Maruyama, M. Tanaka, Proc. 22<sup>nd</sup> EUPVSEC (2007) 932.
- [4] N. Brinkmann, G. Micard, Y. Schiele, G. Hahn, B. Terheiden, Phys. Stat. Sol. RRL 7 (2013) 322.
- [5] S. Dauwe, J. Schmidt, R. Hezel, Proc. 29<sup>th</sup> IEEE

- PVSC (2002) 1246.
- [6] A. Descoeurdes, L. Barraud, R. Bartlome, G. Choong, S. De Wolf, F. Zicarelli, C. Ballif, *Appl. Phys. Lett.* 97 (2010) 183505.
  - [7] D. Pysch, M. Bivour, K. Zimmermann, C. Schetter, M. Hermle, S.W. Glunz, *Proc. 24<sup>th</sup> EUPVSEC* (2009) 1580.
  - [8] M.J. Kushner, *J. Appl. Phys.* 63 (1988) 2532.
  - [9] A. Chowdhury, S. Mukhowadhyay, S. Ray, *Sol. En. Mat. Sol. C.* 94 (2010) 1522.
  - [10] P. Kounavis, D. Mataras, N. Spiliopoulos, E. Mytilineou, D. Rapakoulias, *J. Appl. Phys.* 75 (1994) 1599.
  - [11] R.C. Ross, J. Jaklik, *J. Appl. Phys.* 55 (1984) 3785.
  - [12] S. Ishihara, M. Kitagawa, T. Hirao, K. Wasa, T. Arita, K. Mori, *J. Appl. Phys.* 62 (1987) 485.
  - [13] N. Brinkmann, A. Gorgulla, A. Bauer, D. Skorka, G. Micard, G. Hahn, B. Terheiden, to be submitted.
  - [14] F.A. Bogenschuetz, *Aetzpraxis fuer Halbleiter*, Hanser, Munich, 1967.
  - [15] W. Kern, *J. Electrochemical Society* 137 (1990) 1892.
  - [16] R.A. Sinton, A. Cuevas, *Appl. Phys. Lett.* 69 (1996) 2510.
  - [17] S. Olibet, E. Vallat-Sauvain, C. Ballif, *Phys. Rev. B* 76 (2007) 35326-1.
  - [18] M. Fox, *Optical Properties of Solids*, Oxford University Press, 2010.
  - [19] J. Tauc, A. Menth, *J. Non-Crystl. Solids* 8 (1972) 569.
  - [20] A.A. Langford, M.L. Fleet, B.P. Nelson, W.A. Lanford, N. Maley, *Phys. Rev. B* 45 (1992) 13367.